INTERFACE

rsif.royalsocietypublishing.org

Research

Cite this article: Hechenleitner EM, Grellet-Tinner G, Foley M, Fiorelli LE, Thompson MB. 2016 Micro-CT scan reveals an unexpected high-volume and interconnected pore network in a Cretaceous Sanagasta dinosaur eggshell. *J. R. Soc. Interface* **13**: 20160008.
http://dx.doi.org/10.1098/rsif.2016.0008

Received: 4 January 2016
Accepted: 29 February 2016

Subject Category:
Life Sciences–Earth Science interface

Subject Areas:
biomechanics, evolution, biometrics

Keywords:
titanosaurs, hydrothermal incubation, burrow-nesting, Sanagasta, micro-CT

Author for correspondence:
E. Martín Hechenleitner
e-mail: emhechenleitner@gmail.com, ehechenleitner@crilar-conicet.gob.ar

Electronic supplementary material is available at http://dx.doi.org/10.1098/rsif.2016.0008 or via http://rsif.royalsocietypublishing.org.

THE ROYAL SOCIETY PUBLISHING

Micro-CT scan reveals an unexpected high-volume and interconnected pore network in a Cretaceous Sanagasta dinosaur eggshell

E. Martín Hechenleitner[1], Gerald Grellet-Tinner[1,2], Matthew Foley[3], Lucas E. Fiorelli[1] and Michael B. Thompson[4]

[1]Centro Regional de Investigaciones Científicas y Transferencia Tecnológica de La Rioja (CRILAR-CONICET), Entre Ríos y Mendoza s/n., Anillaco 5301, La Rioja, Argentina
[2]Orcas Island Historical Museum, Eastsound, Washington DC, USA
[3]Australian Centre for Microscopy and Microanalysis, and [4]School of Biological Sciences (A08), University of Sydney, New South Wales 2006, Australia

EMH, 0000-0002-9538-5681; LEF, 0000-0001-5254-6935

The Cretaceous Sanagasta neosauropod nesting site (La Rioja, Argentina) was the first confirmed instance of extinct dinosaurs using geothermal-generated heat to incubate their eggs. The nesting strategy and hydrothermal activities at this site led to the conclusion that the surprisingly 7 mm thick-shelled eggs were adapted to harsh hydrothermal microenvironments. We used micro-CT scans in this study to obtain the first three-dimensional microcharacterization of these eggshells. Micro-CT-based analyses provide a robust assessment of gas conductance in fossil dinosaur eggshells with complex pore canal systems, allowing calculation, for the first time, of the shell conductance through its thickness. This novel approach suggests that the shell conductance could have risen during incubation to seven times more than previously estimated as the eggshell erodes. In addition, micro-CT observations reveal that the constant widening and branching of pore canals form a complex funnel-like pore canal system. Furthermore, the high density of pore canals and the presence of a lateral canal network in the shell reduce the risks of pore obstruction during the extended incubation of these eggs in a relatively highly humid and muddy nesting environment.

1. Introduction

Titanosaurs were Mesozoic mega-herbivorous dinosaurs that inhabited all the land masses. However, the unequivocal record of their nesting sites is to date limited to South America, Europe and Asia [1]. The study of their eggs and eggshells has recently provided new insights on their intriguing palaeobiology, suggesting that these long-necked behemoths were warm-blooded animals that selected globally distributed but highly particular nesting sites, using mound-building and burrow-nesting strategies to incubate their eggs [1–4].

The Sanagasta nesting site (La Rioja, Argentina) was the first, but not the only [1,3,5], confirmed case of extinct dinosaurs incubating their eggs with geothermal-generated heat [2]. The synchronicity between the oviposition and the hydrothermal activities led Grellet-Tinner & Fiorelli [2] to conclude that the Sanagasta eggs were adapted to harsh hydrothermal nesting environments. However, due to methodological limitations (i.e. eggshells are typically studied using destructive thin sections that greatly hinder the understanding of their three-dimensional morphology), it was impossible to understand the physiological impact of the thinning of their surprisingly thick-shelled eggs due to erosion by the geothermal pore fluids.

Here we report the first micro-CT-based three-dimensional reconstruction and microcharacterization of any sauropod dinosaur eggshell. The new

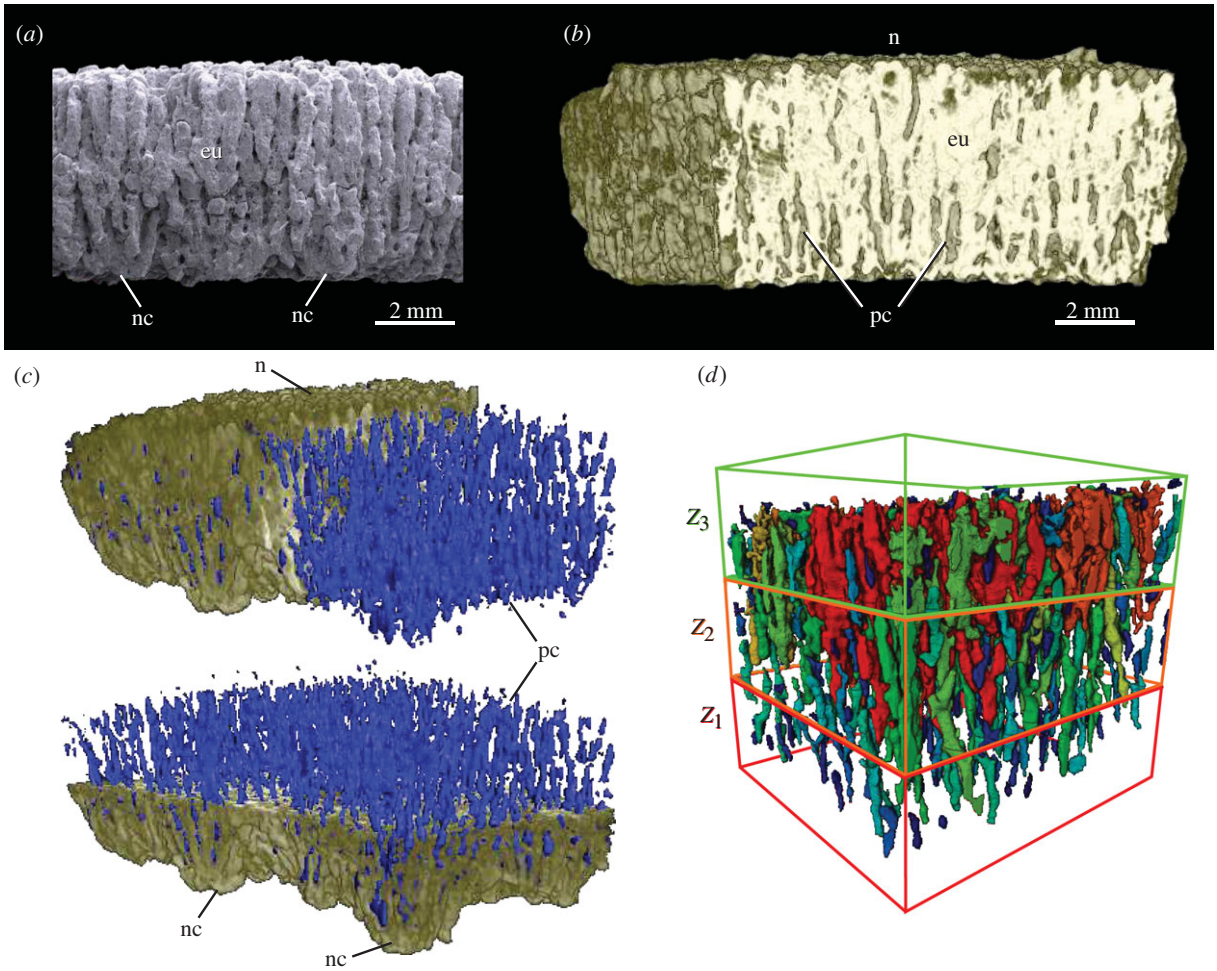

Figure 1. Sanagasta eggshell in radial view. (*a*) Scanning electron microscope image, (*b*) micro-CT-based reconstruction, (*c*) general view of the eggshell and its pore canal system (highlighted in blue in the online version) and (*d*) pore canal system showing the shell segmentation in three concentric zones: Z_1–Z_3. Different grey tones (colours in the online version) were used in an attempt to individualize pore canals. eu, eggshell unit; n, node on the outer shell surface; nc, nucleation centre; pc, pore canal. (Online version in colour.)

three-dimensional analyses provide a robust assessment of gas conductance in the Sanagasta eggshells, allowing for the first time the calculation, rather than an estimation, of gas conductance of these titanosaur eggshells.

2. Results

Microcharacterizations based on three-dimensional reconstructions of a pristine 5.6 mm thick eggshell (figure 1*a*,*b*) from the Sanagasta nesting site indicate that it consists of a single thick structural layer, displaying well-defined units formed by calcite crystals radiating from nucleation centres (figure 1*c*). On average, more than 20% of the shell volume consists of voids (empty spaces). Such a feature has not previously been noticed in the eggshells of extinct dinosaurs and is interesting because of the potential effect of the voids on the mechanical resistance and gas diffusion of these shells.

The concentration and lateral connection of the pore canals define three distinct eggshell zones (Z_{1-3}; figure 1*d*). Z_1, the innermost third of the shell, is radially crossed by multiple vertical and straight pore canals that are closely aligned and parallel to each other, reaching 10% of the volume in this zone. Their diameter narrows through the first approximately 0.5 mm but then widens towards the shell's external surface, producing a slight but noticeable increase in the proportion of voids across this portion of the shell. Although the pore canal ramifications are visible throughout the shell thickness, they occur more frequently in the outer two-thirds of the eggshell (figure 2*a*). In Z_2, the straight pore canals widen in cross section and branch frequently into lateral interconnections (electronic supplementary material, S1), gradually increasing the proportion of voids outwards, duplicating that of Z_1. Lastly, in Z_3, the pore canals branch into two or more subcanals of nearly comparable diameters (figure 2*b*). As branching occurs, pore canals increasingly interconnect laterally, vertically and at random angles (figure 2*a*,*b*), forming a lateral canal network that sharply increases the concentration and number of canals. This constitutes the most porous section of the eggshell, containing up to 57% of its total void volume.

The total egg pore canal area (A_p) calculated at tangential intervals of 20.3 µm indicates a sharp increase outwards (figure 3*a*), driven by the gradual widening of the pores in addition to their constant branching. Thus, the entire pore canal system could be modelled as a funnel-shaped structure [6,7]. We calculated pore-diffusive resistance and its reciprocal conductance to water vapour [6] of each of the same 20.3 µm thick segments, mirroring the shell thinning process during incubation (electronic supplementary material, S2; Material and methods), as previously reported [2,5]. Considering circular cross sections we obtained the diffusive resistances at each segment (figure 3*b*) based on Fick's first law, and boundary layer resistance at the inner apertures based on Stefan's law [6–8]. In accordance with Tøien

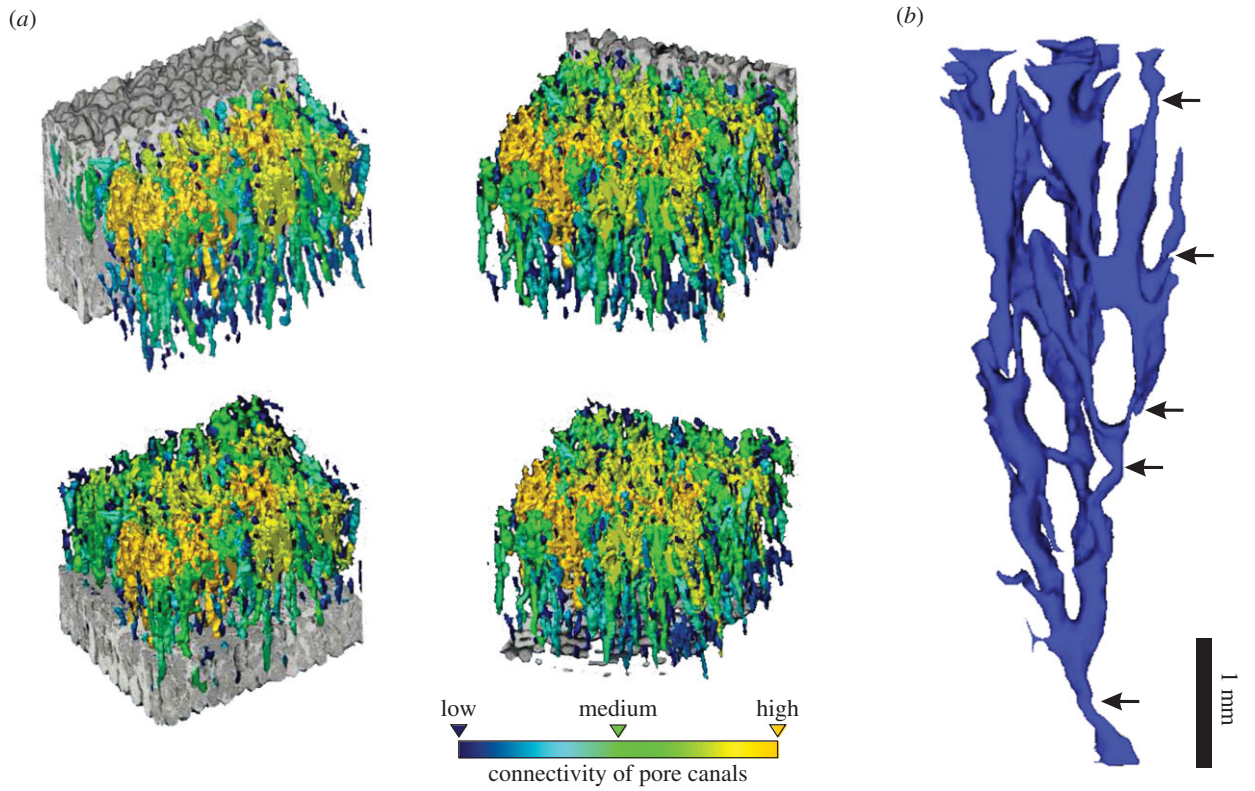

Figure 2. Pore canal system and pore set. (*a*) Pore canal system showing the high degree of lateral interconnection. The canals are coloured according to a connectivity gradient. See electronic supplementary material, S1. (*b*) Restoration of a pore set. Several branches were deliberately cut to enhance viewing. Note that pore canal constrictions appear in different branches at any depth (arrows). (Online version in colour.)

et al. [6,8] (but contra Simkiss [7]) our calculations indicate a very low inner aperture effect, from 0.8% to 2.1% through eggshell thinning. As the diffusive resistances of each segment are cumulative [6], we calculated total egg water vapour conductance (G_{H2O}; figure 3*c*, coloured blue in the online version). The results (electronic supplementary material, S2) indicate that the shell conductance grows only a little through Z_{3-2} compared with the exponential increase experienced when shell thickness reduces below approximately 2.2 mm thick (Z_1).

To compare our results with previous studies [5], we calculated egg G_{H2O} by using the equation derived from Fick's first law of gas diffusion (see Material and methods). Here, we considered only the outermost tangential section for each thickness, thus assuming single straight pore canals (figure 3*c*, coloured orange in the online version; electronic supplementary material, S2). This way, the results present a much more erratic pattern throughout Z_{2-3}, with sudden surges and falls of conductance.

3. Discussion

The Sanagasta eggs (approx. 4850 cm^3) are more than 1.5 times larger than those of other titanosaurs [1,5], paralleling the size difference between megapode eggs (e.g. *Alectura lathami* and *Leipoa ocellata*) and other galliformes of comparable body size [9]. Such larger eggs allow storage of more nutrients for prolonged incubation and hatching of hyperprecocial chicks [10,11]. Despite the difference in egg size, several morphological features of Z_1 are strikingly reminiscent of the Auca Mahuevo titanosaur eggshells [12], including their Y-shaped pore canals (figure 3*d*). Typically, these eggshells are thinner than 1–1.2 mm at the time embryos hatch because their inner surface thins during embryogenesis [12–19] and the outer surface is eroded as a direct consequence of their incubation in burial conditions with ambient heat and moisture [1,5,12,20] in contrast with the classic avian contact incubation. In addition, calcium absorption from the inner surface of the eggshell is typically 4–8% during embryonic development in birds, but it is much higher (12–21%) in megapodes, which bury their eggs [15–17,19] like the titanosaurs [1]. Although clearly the percentage of shell thinning does not scale isometrically with shell thickness, inner-shell thinning has been observed in the Sanagasta eggshells [5]. Moreover, the geochemical analyses of the Sanagasta nesting sediments coupled with the wide range of eggshell thicknesses [2,21] independently support the hypothesis that the hydrothermal fluids progressively and greatly eroded the outer surface of the 7.9 mm thick eggshell during incubation [2,5,21,22]. This chemical erosion represents the main factor contributing to the shell final thickness of 1.2 mm [2,5,22] that allows an embryo to successfully break through at hatching time.

This study confirms that the pore canal system of the Sanagasta titanosaur eggshells have the most complex pattern known to date (figure 2*a*). Pore canals can at best be individualized into small sets due to their high density and multiple lateral interconnections (e.g. figure 2*b*). Moreover, a given pore set and its branches vary greatly and randomly in diameter throughout the eggshell thickness (e.g. arrows in figure 2*b*), hence hindering the accurate determination of the smallest cross sections that potentially restrict gas diffusion during shell thinning. Therefore, these features represent a notable hurdle to the generalization of A_p, typically used to estimate the conductance of fossil eggshells. Owing

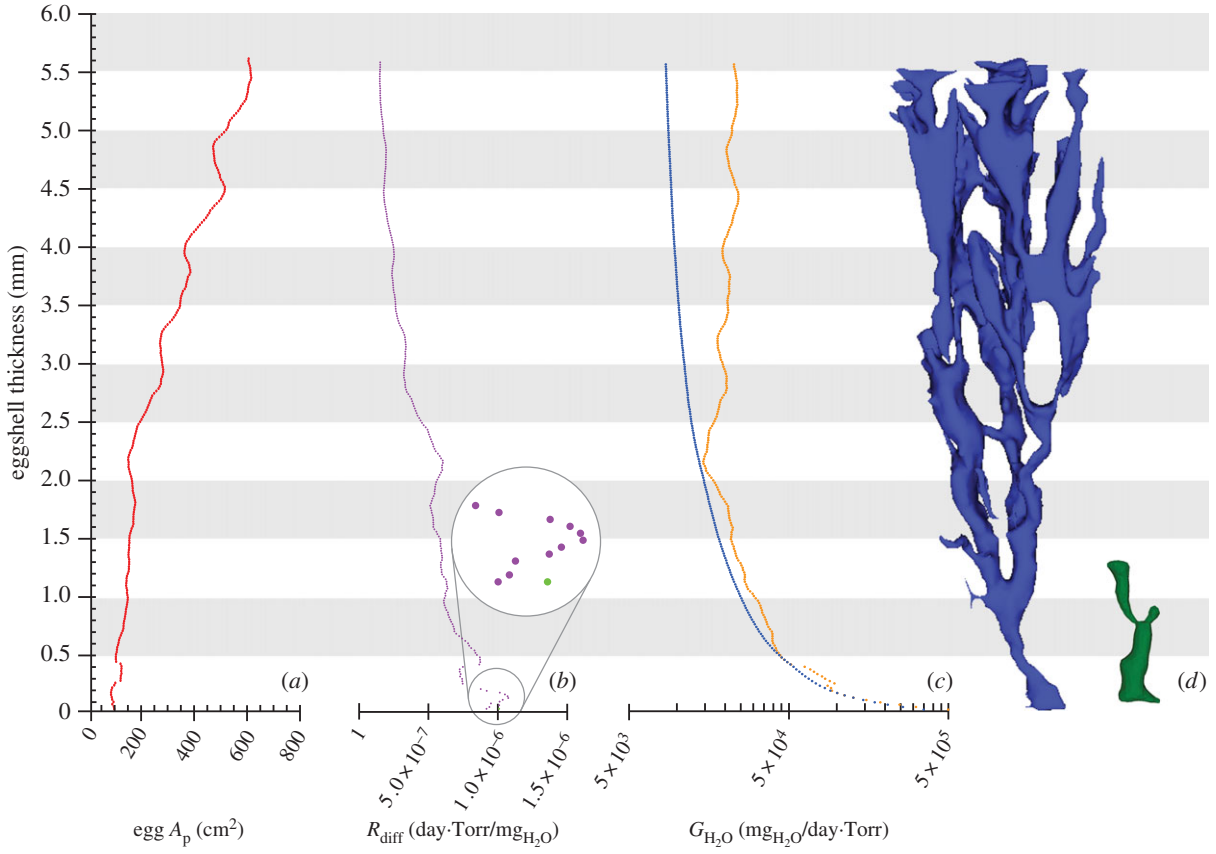

Figure 3. Egg pore area (A_p), diffusive resistance (R_{diff}) and water vapour conductance (G_{H2O}) variation through the shell thinning of a 5.6 mm eggshell from Sanagasta. (*a*) A_p of each shell segment. (*b*) R_{diff} of each shell segment (dark grey; purple in the online version; based on Fick's law) and the inner aperture (light grey; green in the online version; based on Stefan's law). (*c*) G_{H2O} at each thickness estimated through equation (4.1) (light grey; orange in the online version) and derived from R_{diff} (dark grey; blue in the online version); see Material and methods. Data are listed in the electronic supplementary material, S2. (*d*) Scaled Sanagasta pore set (left) and Auca Mahuevo layer 4 pore canal (right). Restoration of the Auca Mahuevo pore canal based on Grellet-Tinner *et al.* [5]. (Online version in colour.)

to the pore canal system complexity, G_{H2O} calculations of the Sanagasta and probably other titanosaur eggshells using single tangential sections may lead to significantly disparate estimates (figure 3*c*), questioning the effectiveness of the previously used methods for estimating the humidity in nesting microenvironments of extinct dinosaurs with complex pore canal systems in their eggshells. By contrast, the use of micro-CT scans allows diffusive resistance and G_{H2O} to be accurately calculated in such conditions.

The high degree of lateral interconnection allows the pore canal system to be considered as a unit which can be interpreted as a funnel-shaped structure due to its total A_p increase from the inside out of the shell. Overall, our observations indicate that the Sanagasta shell's narrowest A_p (i.e. the section where the narrowest cross sections are expected) is close to the inner-shell surface (figure 3*a*), as typically observed in megapode and other sauropod eggshells [6,15,19,23,24]. As such, the G_{H2O} measured through shell thinning mirrors that of modern megapode eggs [15–17], rising exponentially into the last third of the incubation period (figure 3*c*). Considering that most of the diffusive resistance is concentrated at the innermost Z_1, the subtle but constant increase in conductance during removal of Z_{3-2} must be driven by the strong thickness component of these titanosaur eggshells.

While the Sanagasta eggshells exhibit the most complex lateral canal network so far described, lateral interconnection among vertical pore canals was previously noted in thinner sauropod eggshells [24,25] and, at least, one species of modern megapodes. Two species of mound-building megapodes, the brush-turkey (*A. lathami*) and the malleefowl (*L. ocellata*), show differences in their nesting strategies, the brush-turkeys incubating eggs in mound-nests with high relative humidities and malleefowl eggs incubating in dry nests (G Grellet-Tinner 2014, unpublished data). The Y-shaped pores in the eggshells is a shared character of both species, but the single or double horizontal connections between adjacent pores are particular to *A. lathami* (G Grellet-Tinner 2014, unpublished data). Based on present observations, they would facilitate the lateral diffusion of gases in the event of occlusion of pores on the surface of the egg. Such occlusion is more likely in buried eggs than in eggs incubated in open nests, especially those of brush-turkey, where the nest mound is composed predominantly of moist vegetable matter [16].

Knowing that the Sanagasta egg clutches were deposited in close proximity to hydrothermal structures such as vents, springs and pools [1,2,5,21,22], water and muddy material could have easily obstructed several pores at times [16]. Although the lateral canal network is well developed in Z_{3-2}, it greatly reduces in Z_1 (electronic supplementary material, S1), where pore canal obstructions should not have represented a drawback because shell thinning leads to a net increase (double) in the shell's conductance in a few tenths of a millimetre (figure 3*c*). Therefore, the presence of a highly complex lateral network at the outermost two-thirds of the eggshell reinforces previous hypotheses that suggest that the Sanagasta eggs were able to maintain a sufficient gas and water vapour diffusion through their

shell during burial incubation even in the event of partial obstruction [1,2,5].

The extremely thick Sanagasta eggshells were well adapted to minimize the effects of chemical erosion and obstruction of pores by possessing the most complex funnel-like pore canal system so far described. This complex pore system indicates that the gas conductance of these 7.9 mm thick eggshells could have increased up to seven times more than previously estimated [5]. Funnel-shaped pores are extremely important evolutionarily as their low resistance to diffusion allows dissociation of the constraints imposed by respiration from those related to the eggshell size and strength [7]. The presence of a funnel-like pore canal system may have permitted the extremely thick Sanagasta eggshells to act as a mechanism to counteract the external acid erosion in this hydrothermal nesting strategy.

Lastly, the new data demonstrate that gas exchange estimations for sauropod eggs based on the equation derived from Fick's first law using single tangential sections are perhaps an oversimplification for fossil dinosaur eggshells with such complex pore canal systems as observed in the Sanagasta samples.

4. Material and methods

(a) Materials

Fossil eggshells CRILAR-Pv 406, housed at the Centro Regional de Investigaciones Científicas y Transferencia Tecnológica de La Rioja (CRILAR-CONICET), were recovered at sub-site G of the Sanagasta nesting site in La Rioja province, northwest Argentina [2].

(b) Scanning electron microscope imaging

The scanning electron microscope analysis and preparation of eggshell samples were carried out in accordance with Grellet-Tinner's methodology [13]. Observations were carried out with a Philips® Scanning Electron Microscope XL 30 at the Microscopy Laboratory of the Museo Argentino de Ciencias Naturales 'Bernardino Rivadavia', Buenos Aires, Argentina.

(c) Micro-CT scanning and analysis

Micro-CT microcharacterizations were performed at the Australian Centre for Microscopy and Microanalysis, University of Sydney, Australia. The eggshell specimens were scanned using an Xradia MicroXCT-400 system operating at 55–60 keV and 127–133 mA. The specimens were mounted in low-density polystyrene to prevent movement during their 360° rotation with projections collected at 0.2° intervals. Geometric and objective magnification was used to scan the Sanagasta samples at a voxel resolution of 20.3 µm. Reconstructed image stacks were rendered using Avizo Fire (VSG|FEI Visualization Sciences Group) with the internal pore networks segmented using built-in thresholding functions following a nonlinear filtering of the dataset to reduce image noise. Pore volume calculations were obtained by running a material calculation on the samples with each voxel being assigned to one of pore, shell or exterior (air) based on the attenuation of the X-ray beam.

(d) Conductance calculations

A section of 44.1 mm^2 of a pristine 5.6 mm thick eggshell was used to make volumetric calculations. As a voxel measures 20.3 µm on each side, the sample was divided in 275 tangential segments. It is noteworthy that, given the size of the specimen, the effect of the curvature of the egg is negligible. Pore length (L_s) was considered to be equal to eggshell thickness in all the calculations.

To allow the comparison of our results with previous studies, G_{H2O} of the Sanagasta eggshells was also estimated through the most frequently used formula [5,9,26,27]:

$$G_{H2O} = \frac{A_p}{0.478 \cdot L_s}, \tag{4.1}$$

where A_p is the total pore area of the egg (mm^2), L_s is the pore length (mm) and the constant in the formula is linked to a nesting temperature of 25°C. Although we suspect that the nesting temperature at Sanagasta was above 25°C, this value is widely used in the literature [5–9,16,27–30]. Thus, it allows further comparison with fossil and extant dinosaur eggs and eggshells. Results obtained from the latter (plotted in figure 3*c*, orange in the online version) were calculated by using only A_p of the outermost tangential segment for each thickness (e.g. 147.8 $cm^2\ egg^{-1}$ at 1 mm thick).

Considering the oversimplification of the latter calculations, the volumetric data were also used to evaluate the diffusive resistance of the inner pore apertures (based on Stefan's law) and each of the 275 shell segments (based on Fick's first law). G_{H2O} of each segment was derived from these calculations, according to Tøien *et al.* [6].

Authors' contributions. E.M.H. and G.G.-T. designed the study, performed comparative work and co-wrote the paper; E.M.H. also carried out the data analysis; M.F. collected data, and with L.E.F. and M.B.T. contributed to the writing and discussion.

Competing interests. We declare we have no competing interests.

Funding. Research funded by CONICET, the Jurassic Foundation (to E.M.H.), the Agencia Nacional de Promoción Científica y Tecnológica (PICT 2012-0421 to L.E.F.) and COFECyT (Asetur 2010 to L.E.F.). Analytic work supported by the University of Sydney International Fellowship (to G.G.-T.).

Acknowledgements. The authors acknowledge the facilities and the scientific and technical assistance of the Australian Microscopy & Microanalysis Research Facility at the Australian Centre for Microscopy & Microanalysis at the University of Sydney, and the Secretaría de Cultura de La Rioja (Argentina) and S. de la Vega and C. Bustamante (CRILAR-CONICET) for their help and support. E.M.H. thanks L. Leuzinger, S. Rocher and M. Macchioli Grande for discussions and comments on this manuscript and acknowledges the CONICET doctoral fellowship for supporting his studies. G.G.-T. is grateful for the support of the School of Biology and the ACMM of the University of Sydney.

References

1. Hechenleitner EM, Grellet-Tinner G, Fiorelli LE. 2015 What do giant titanosaur dinosaurs and modern Australasian megapodes have in common? *PeerJ* **3**, e1341. (doi:10.7717/peerj.1341)
2. Grellet-Tinner G, Fiorelli LE. 2010 A new Argentinean nesting site showing neosauropod dinosaur reproduction in a Cretaceous hydrothermal environment. *Nat. Commun.* **1**, 32. (doi:10.1038/ncomms1031)
3. Grellet-Tinner G, Codrea V, Folie A, Higa A, Smith T. 2012 First evidence of reproductive adaptation to 'island effect' of a dwarf Cretaceous Romanian titanosaur, with embryonic integument in ovo. *PLoS ONE* **7**, e32051. (doi:10.1371/journal.pone.0032051)
4. Eagle RA *et al.* 2015 Isotopic ordering in eggshells reflects body temperatures and suggests differing thermophysiology in two Cretaceous dinosaurs. *Nat. Commun.* **6**, 8296. (doi:10.1038/ncomms9296)

5. Grellet-Tinner G, Fiorelli LE, Salvador RB. 2012 Water vapor conductance of the Lower Cretaceous dinosaurian eggs from Sanagasta, La Rioja, Argentina: paleobiological and paleoecological implications for South American faveoloolithid and megaloolithid eggs. *Palaios* **27**, 35–47. (doi:10.2110/palo.2011.p11-061r)
6. Tøien Ø, Paganelli CV, Rahn H, Johnson RR. 1988 Diffusive resistance of avian eggshell pores. *Respir. Physiol*. **74**, 345–354. (doi:10.1016/0034-5687(88)90042-4)
7. Simkiss K. 1986 Eggshell conductance—Fick's or Stefan's law? *Respir. Physiol*. **65**, 213–222. (doi:10.1016/0034-5687(86)90051-4)
8. Tøien Ø, Paganelli CV, Rahn H, Johnson RR. 1987 Influence of eggshell pore shape on gas diffusion. *J. Exp. Zool. Suppl*. **1**, 181–186.
9. Ar A, Rahn H. 1985 Pores in avian eggshells: gas conductance, gas exchange and embryonic growth rate. *Respir. Physiol*. **61**, 1–20. (doi:10.1016/0034-5687(85)90024-6)
10. Vleck D, Vleck CM, Seymour RS. 1984 Energetics of embryonic development in the megapode birds, mallee fowl Leipoa ocellata and brush turkey Alectura lathami. *Physiol. Zool*. **57**, 444–456. (doi:10.1086/physzool.57.4.30163346)
11. Eiby YA, Booth DT. 2009 The effects of incubation temperature on the morphology and composition of Australian brush-turkey (*Alectura lathami*) chicks. *J. Comp. Physiol. B* **179**, 875–882. (doi:10.1007/s00360-009-0370-4)
12. Grellet-Tinner G, Chiappe LM, Coria RA. 2004 Eggs of titanosaurid sauropods from the Upper Cretaceous of Auca Mahuevo (Argentina). *Can. J. Earth Sci*. **41**, 949–960. (doi:10.1139/E04-049)
13. Grellet-Tinner G. 2006 Phylogenetic interpretation of eggs and eggshells: implications for phylogeny of Palaeognathae. *Alcheringa* **30**, 141–182. (doi:10.1080/03115510608619350)
14. Board RG, Sparks NH. 1991 Shell structure and formation in avian eggs. In *Egg incubation: its effects on embryonic development in birds and reptiles*, pp. 71–86. Cambridge, UK: Cambridge University Press.
15. Booth DT, Seymour RS. 1987 Effect of eggshell thinning on water vapor conductance of malleefowl eggs. *Condor* **89**, 453–459. (doi:10.2307/1368635)
16. Seymour RS, Vleck D, Vleck CM, Booth DT. 1987 Water relations of buried eggs of mound building birds. *J. Comp. Physiol. B* **157**, 413–422. (doi:10.1007/BF00691824)
17. Booth DT, Thompson MB. 1991 A comparison of reptilian eggs with those of megapode birds. In *Egg incubation: its effects on embryonic development in birds and reptiles* (eds DC Deeming, MWJ Ferguson), pp. 325–344. Cambridge, UK: Cambridge University Press.
18. Packard MJ, DeMarco VG. 1991 Eggshell ultrastructure and formation in eggs of oviparous reptiles. In *Egg incubation: its effects on embryonic development in birds and reptiles* (eds DC Deeming, MWJ Ferguson), pp. 53–69. Cambridge, UK: Cambridge University Press.
19. Booth D. 1989 Regional changes in shell thickness, shell conductance, and pore structure during incubation in eggs of the mute swan. *Physiol. Zool*. **62**, 607–620. (doi:10.1086/physzool.62.2.30156188)
20. Clayburn JK, Smith DL, Hayward JL. 2004 Taphonomic effects of pH and temperature on extant avian dinosaur eggshell. *Palaios* **19**, 170–177. (doi:10.1669/0883-1351(2004)019<0170:TEOPAT>2.0.CO;2)
21. Fiorelli LE, Grellet-Tinner G, Alasino PH, Argañaraz E. 2012 The geology and palaeoecology of the newly discovered Cretaceous neosauropod hydrothermal nesting site in Sanagasta (Los Llanos Formation), La Rioja, northwest Argentina. *Cretac. Res*. **35**, 94–117. (doi:10.1016/j.cretres.2011.12.002)
22. Fiorelli LE, Grellet-Tinner G, Argarañaz E, Salgado L. 2013 Tafonomía del sitio de nidificación de neosaurópodos de Sanagasta (La Rioja, Argentina): ejemplo de preservación excepcional en un paleoambiente hidrotermal del Cretácico. *Ameghiniana* **50**, 389–406. (doi:10.5710/AMGH.15.11.2012.523)
23. Deeming DC, Thompson MB. 1991 Gas exchange across reptilian eggshells. In *Egg incubation: its effects on embryonic development in birds and reptiles* (eds DC Deeming, MWJ Ferguson), pp. 277–284. Cambridge, UK: Cambridge University Press.
24. Williams DLG, Seymour RS, Kerourio P. 1984 Structure of fossil dinosaur eggshell from the Aix Basin, France. *Palaeogeogr. Palaeoclimatol. Palaeoecol*. **45**, 23–37. (doi:10.1016/0031-0182(84)90107-X)
25. Argañaraz E, Grellet-Tinner G, Fiorelli LE, Krause LM, Rauhut OWH. 2013 Huevos de saurópodos del Aptiano–Albiano, Formación Cerro Barcino (Patagonia, Argentina): Un enigma paleoambiental y paleobiológico. *Ameghiniana* **50**, 33–50. (doi:10.5710/AMGH.9.11.2012.551)
26. Paganelli CV. 1980 The physics of gas exchange across the avian eggshell. *Am. Zool*. **20**, 329–338. (doi:10.1093/icb/20.2.329)
27. Deeming DC. 2006 Ultrastructural and functional morphology of eggshells supports the idea that dinosaur eggs were incubated buried in a substrate. *Palaeontology* **49**, 171–185. (doi:10.1111/j.1475-4983.2005.00536.x)
28. Ar A, Paganelli CV, Reeves RB, Greene DG, Rahn H. 1974 The avian egg: water vapor conductance, shell thickness, and functional pore area. *Condor* **76**, 153–158. (doi:10.2307/1366725)
29. Birchard GF, Kilgore DLJ. 1980 Conductance of water vapor in eggs of burrowing and nonburrowing birds: implications for embryonic gas exchange. *Physiol. Zool*. **53**, 284–292. (doi:10.1086/physzool.53.3.30155791)
30. Tanaka K, Zelenitsky DK, Therrien F. 2015 Eggshell porosity provides insight on evolution of nesting in dinosaurs. *PLoS ONE* **10**, e0142829. (doi:10.1371/journal.pone.0142829)